Analytical prediction of springback based on residual differential strain during sheet metal bending

H K Yi[1], **D W Kim**[1], **C J Van Tyne**[2], and **Y H Moon**[1*]
[1]Engineering Research Center for Net Shape and Die Manufacturing/Department of Mechanical Engineering, Pusan National University, Busan, Republic of Korea
[2]Department of Metallurgical and Materials Engineering, Colorado School of Mines, Golden, Colorado, USA

The manuscript was received on 30 March 2007 and was accepted after revision for publication on 11 September 2007.

DOI: 10.1243/09544062JMES682

Abstract: As the springback of sheet metal during unloading may cause deviation from a desired shape, accurately predicting springback is essential for the design of sheet stamping operations. Finite-element models have not been successful in predicting springback; hence there is a need for analytical models to make such predictions. In this study, a model based on differential strains after relief from the maximum bending stress is derived for six different deformation patterns in order to predict springback analytically. The springback for each deformation pattern is estimated by the residual differential strains between outer and inner surfaces after elastic recovery. Each of the six deformation patterns has a valid region of applicability, based on elastic modulus, yield strength, applied tension, and bending geometry. Analytical equations for the springback of the sheet deformed under these six deformation patterns are derived. Traditional analytical models for springback prediction have been based on elastic unloading from a bending moment. Traditional models also require the knowledge of the stress distribution through the thickness of the sheet, whereas the residual differential strain model only requires the stress state on the outer and inner surfaces of the sheet. In order to compare the residual differential strain model with the traditional bending moment model, a bending moment model is derived for the same exact deformation patterns. Results from the two models are compared for various materials.

Keywords: springback, sheet metal forming, analytical model, residual differential strain, bending moment model, multiple deformation patterns

1 INTRODUCTION

Springback refers to the elastic recovery of deformed parts. Springback occurs because of the elastic relief from the bending moment imparted to the sheet metal during forming. Springback is common and inevitable in each stage of the production process where the material undergoes geometrical changes. Accordingly, factors related to the generation of stress in the material during loading and unloading processes influence the springback behaviour of press-formed parts [**1**–**4**].

The application of high strength steels and aluminium to automotive sheet components is increasing, as they effectively reduce body weight while keeping and improving structural performance [**5**, **6**]. Unfortunately, these materials tend to have a larger springback than mild steels. The high values of the ratio of strength to Young's modulus result in more springback. For a given amount of deformation, higher strength materials (e.g. high strength steels) will unload from a higher strength, resulting in more elastic unloading strain. Likewise, for a material with a lower Young's modulus (e.g. aluminium alloys), the amount of elastic unloading strain, which causes the springback, is higher. Overall, it is

Corresponding author: Engineering Research Center for Net Shape and Die Manufacturing, Department of Mechanical Engineering, Pusan National University, San 30, Jangjeon-dong, Geumjeong-gu, Busan 609-735, Republic of Korea. email: yhmoon@pusan.ac.kr

more difficult to accurately produce a part shape without proper springback compensation. As springback is strongly dependent on the part geometry and the materials used, it is not possible to give a general rule of thumb for its compensation. Commercial finite-element programme for sheet forming simulation give good results in terms of formability, strain distribution, and wrinkling – but springback remains a phenomenon often reported as being difficult to simulate. There are certain aspects that make springback especially critical for sheet metal forming [**6**–**10**]. Even small angular springback in deep drawn structures may cause large spatial deformations and distortions of the whole part. As finite-element simulations are computationally intense, efficient analytical methods to predict springback have also been developed [**11**–**13**].

In this study, a model based on differential strains after relief from the maximum bending stress [**14**, **15**] is derived for multiple deformation patterns (i.e. different stress conditions) in order to predict springback analytically. The springback for each deformation pattern is estimated by the residual differential strains between outer and inner surfaces after elastic recovery. As the springback of sheet metal after bending is strongly dependent on the stress state of the deformed sheet, six different deformation patterns, each having a valid region of applicability, are derived on the basis of material parameters (elastic modulus and yield strength), applied tension, and bending geometry. Analytical equations for the springback of the sheet deformed under these six deformation patterns are derived.

Traditional analytical models for springback prediction have been based on elastic unloading from a bending moment [**13**, **16**]. Such models are more complicated than the residual differential strain model that is derived in the present study. Traditional models also require the knowledge of the stress distribution within the part under examination, whereas the residual differential strain model only requires the stress state on the outer and inner surfaces of the sheet. In order to compare the residual differential strain model with the traditional bending moment model, a bending moment model is derived for the same exact deformation patterns. Results from the two models are compared for various materials.

2 ANALYTICAL MODELS FOR SPRINGBACK PREDICTION

Consider the bending process as shown in Fig. 1, where a unit width of a continuous sheet is bent to a radius of curvature ρ, and the bend angle is θ.

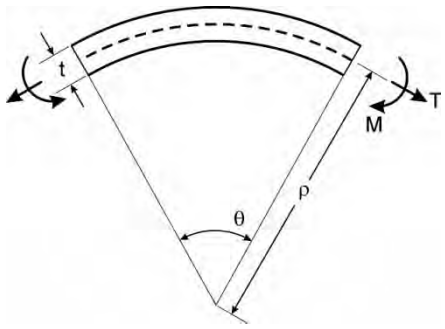

Fig. 1 A unit length of a continuous strip bent along a line

Moment per unit width, M, and tension (force per unit width), T, are applied to the sheet. When the sheet is bent by a pure moment without any tension being applied, the neutral axis will be at the mid-thickness of the sheet. The upper half thickness above neutral axis will be in a tensile stress state, whereas the lower half thickness is in a compressive stress state. In pure bending, the maximum strain occurs in the outer (upper) surface, and the elastic–plastic behaviour at this region is determined by the material parameters (elastic modulus E and yield strength σ_o) and bending geometry. The strain at the yield point ε_o is

$$\varepsilon_o = \frac{\sigma_o}{E} \tag{1}$$

and the maximum strain applied on the outer surface ε_{max} can be expressed by

$$\varepsilon_{max} = \frac{t}{2\rho} \tag{2}$$

where t is the thickness of the sheet and ρ is the radius of the bend.

When ε_{max} exceeds ε_o, then the outer surface will be in a plastic stress state, but if the reverse is true, then the outer surface will be in an elastic stress state. As the springback of sheet metal after bending is strongly dependent on the stress state of the deformed sheet, the springback parameter S_p is introduced for the precise classification of deformation behaviour by dividing equation (2) by equation (1) to obtain

$$S_p = \frac{\varepsilon_{max}}{\varepsilon_o} = \frac{Et}{2\rho\sigma_o} \tag{3}$$

when S_p is greater than 1, the outer surface will be in a plastic stress state and when S_p is less than 1, the outer surface is in an elastic stress state. Figure 2 schematically shows the classification of the springback parameter.

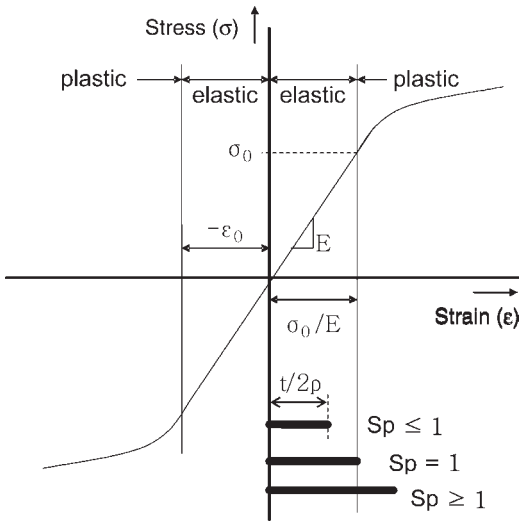

Fig. 2 Classification of springback parameter (S_p)

If the desired curvature of a sheet is less than the limiting elastic curvature, the sheet cannot be formed to shape simply by bending over a die block. It would either springback to the flat shape, or if it were over-bent until it becomes partially plastic, the springback would be so high that the process would be difficult to control. Therefore, in a stamping operation, tension is frequently applied to the sheet, which is first curved elastically to the shape of a die block. For such conditions, the initial moment and the stress state will be changed because of the application of tension.

In the current study, the possible variations of stress states for bent sheet with applied tension are classified on the basis of the amount of the applied strain, ε_a, which originates from applied stress, σ_a. When S_p is less than one, three different deformation patterns are possible, as shown in Table 1 and Fig. 3.

When S_p is greater than one, three different deformation patterns can occur, as shown in Table 2 and Fig. 4. Therefore, six different analytical models are derived – one for each deformation pattern. From the given process conditions and material parameters, the valid deformation pattern is determined first and then the amount of springback can be calculated.

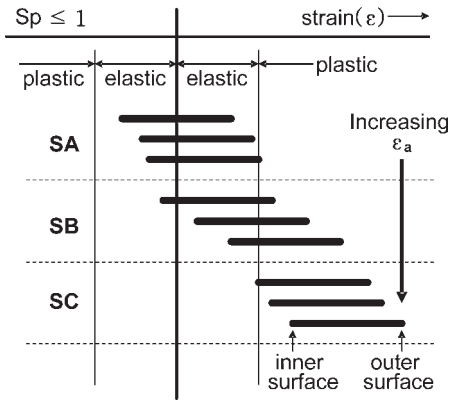

Fig. 3 Possible deformation for given deformation patterns for $S_P \leqslant 1$

2.1 Springback model based on residual differential strain

To date, most analytical springback models have been based on elastic recovery from the applied bending moment that causes the bend. This type of traditional model will be derived in section 2.2. In this section, a model based on the residual differential strain is derived. Differential strain is the difference between the strain on the outer surface of the bend and that on the inner surface of the bend. The residual differential strain method produces simpler analytical equations to determine springback from bending. In addition, the method only requires knowledge of the stress state on the outer and inner surfaces of the bend, rather than the stress distribution through the thickness of the sheet.

Consider the case of a sheet metal bent to radius ρ by applying uniform bending moment. If ρ is such that the maximum stress induced lies within the elastic limit of the material, then on removing the bending moment, the specimen will return to the original shape. However, if ρ is such that the maximum stress induced exceeds the elastic limit of the material, plastic strain will occur at the outer surface and the material will take a permanent set. If on removal of the bending moment, the elastic unloading of the material is not uniform across the thickness, then springback will occur. The bend radius ρ will not be

Table 1 Three possible deformation patterns for $S_p \leqslant 1$ (i.e. $\sigma_0/E \geqslant t/2\rho$)

Inner surface	Outer surface	Valid range	ID
Elastic	Elastic	$\varepsilon_a - t/2\rho \geqslant -\sigma_0/E, \quad \varepsilon_a + t/2\rho \leqslant \sigma_0/E$ $\Rightarrow 0 \leqslant \varepsilon_a \leqslant \sigma_0/E - t/2\rho$	SA
Elastic	Plastic	$\varepsilon_a - t/2\rho \leqslant \sigma_0/E, \quad \varepsilon_a + t/2\rho \geqslant \sigma_0/E$ $\Rightarrow \sigma_0/E - t/2\rho \leqslant \varepsilon_a \leqslant \sigma_0/E + t/2\rho$	SB
Plastic	Plastic	$\varepsilon_a - t/2\rho \geqslant \sigma_0/E, \quad \varepsilon_a + t/2\rho \geqslant \sigma_0/E$ $\Rightarrow \varepsilon_a \geqslant \sigma_0/E + t/2\rho$	SC

Table 2 Three possible deformation patterns for $S_p \geqslant 1$ (i.e. $t/2\rho \geqslant \sigma_0/E$)

Inner surface	Outer surface	Valid range	ID
Plastic	Plastic	$\varepsilon_a - t/2\rho \leqslant -\sigma_0/E, \varepsilon_a + t/2\rho \geqslant \sigma_0/E$ $\Rightarrow \ 0 \leqslant \varepsilon_a \leqslant t/2\rho - \sigma_0/E$	LA
Elastic	Plastic	$\varepsilon_a - t/2\rho \geqslant -\sigma_0/E, \varepsilon_a + t/2\rho \geqslant \sigma_0/E$ $\Rightarrow t/2\rho - \sigma_0/E \leqslant \varepsilon_a \leqslant t/2\rho + \sigma_0/E$	LB
Plastic	Plastic	$\varepsilon_a - t/2\rho \geqslant \sigma_0/E, \quad \varepsilon_a + t/2\rho \geqslant \sigma_0/E$ $\Rightarrow \varepsilon_a \geqslant t/2\rho + \sigma_0/E$	LC

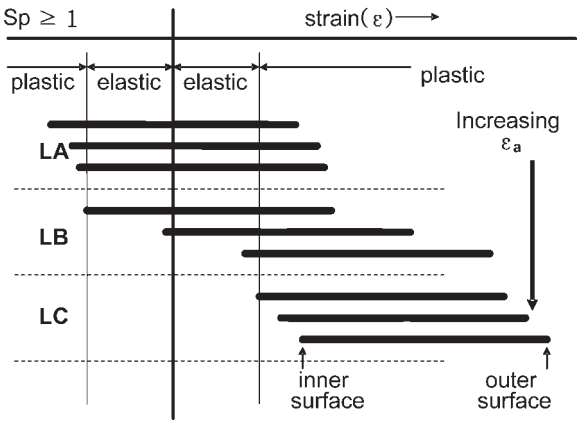

Fig. 4 Possible deformation for given deformation patterns for $S_P \geqslant 1$

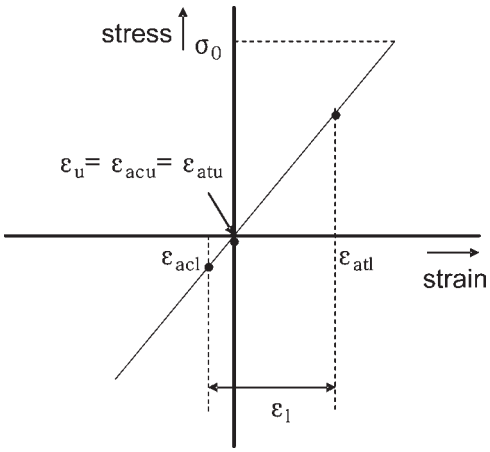

Fig. 5 Stress–strain distribution for deformation pattern 'SA'

maintained in the sheet. Consider a similar specimen that is bent over a rigidly supported die of cylindrical cross-section of radius ρ with a tensile load being applied to each end of the specimen. The tensile stress due to bending is increased and the compressive stress is decreased. As the applied load is increased, the compressive stress is decreased further, and eventually the whole specimen is in tension to a varying degree. Moreover, if the stress on the outer surface (i.e. the surface with the greatest radius) exceeds the elastic limit of the material, the increased applied tension will cause the load to be more evenly distributed throughout the thickness of the material. Eventually, a level of applied load is reached where the stress in the specimen is nearly uniform and the entire sheet thickness is in the plastic range. Removing the applied load, the specimen loses its elastic strain by contracting, and the final radius in the bent sheet can be determined from the residual differential strain.

The springback, SB, for each deformation pattern is estimated by the residual differential strains between outer and inner surfaces of greatest radius after elastic recovery as

$$\mathrm{SB} = \frac{\varepsilon_\mathrm{l} - \varepsilon_\mathrm{u}}{\varepsilon_\mathrm{l}} \tag{4}$$

where ε_l is the strain difference between outer and inner surfaces of greatest radius while loaded and ε_u is the strain difference between outer and inner surfaces of greatest radius after unloading. Because the model is based on residual differential strains in the sheet, springback is defined in terms of strain rather than the traditional measure of angular change.

Figure 5 shows the deformation pattern for 'SA' in which both the inner and outer surfaces are elastic, and the resulting springback is given by

$$\mathrm{SB} = \frac{\varepsilon_\mathrm{l} - \varepsilon_\mathrm{u}}{\varepsilon_\mathrm{l}} = \frac{\varepsilon_\mathrm{l} - 0}{\varepsilon_\mathrm{l}} = 1.0 = 100\% \tag{5}$$

Figure 6 shows the deformation pattern for SB where the inner surface is elastic, whereas the outer surface is plastic, and the resulting springback is given by

$$\mathrm{SB} = \frac{\varepsilon_\mathrm{l} - \varepsilon_\mathrm{u}}{\varepsilon_\mathrm{l}} = \frac{\varepsilon_\mathrm{l} - (\varepsilon_\mathrm{a} + t/2\rho - \sigma_\mathrm{un}/E_\mathrm{un})}{\varepsilon_\mathrm{l}} \tag{6}$$

where E_un is the unloading modulus, ε_a the applied axial strain, and σ_un the strength of the sheet material prior to unloading.

As $\varepsilon_\mathrm{l} = \varepsilon_\mathrm{b} = t/\rho$, where ε_b is the bending strain, then

$$\mathrm{SB} = \frac{t + 2\rho(\sigma_\mathrm{un}/E_\mathrm{un} - \varepsilon_\mathrm{a})}{2t} \tag{7}$$

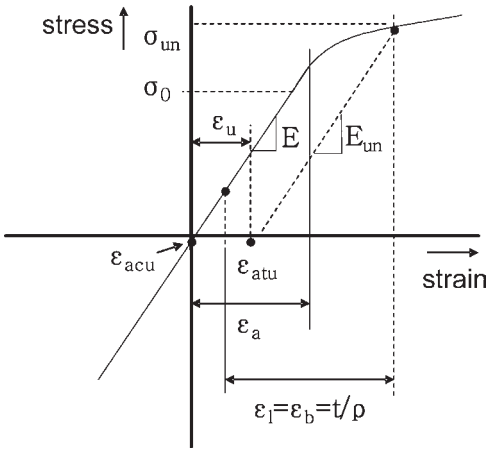

Fig. 6 Stress–strain distribution for deformation pattern SB

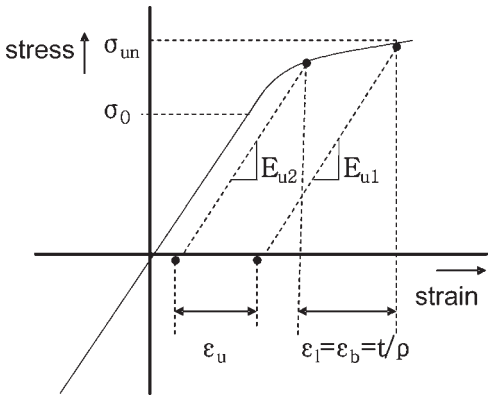

Fig. 7 Stress–strain distribution for deformation pattern SC

The strength of the sheet can be modelled as a power law type of material, so that $\sigma_{un} = K(t/2\rho + \varepsilon_a)^n$, where K is the strength coefficient of the sheet material and n is the strain hardening exponent for the sheet material.

Figure 7 shows the deformation pattern for SC, where both inner and outer surfaces are plastic and the amount of springback is

$$\begin{aligned} SB &= \frac{\varepsilon_l - \varepsilon_u}{\varepsilon_l} \\ &= \frac{t/\rho - (\varepsilon_a + t/2\rho - K(\varepsilon_a + t/2\rho)^n/E_{u1} - [\varepsilon_a - t/2\rho - K(\varepsilon_a - t/2\rho)^n/E_{u2}])}{\varepsilon_l} \\ &= \frac{K\rho[(\varepsilon_a + t/2\rho)^n/E_{u1} - (\varepsilon_a - t/2\rho)^n/E_{u2}]}{t} \end{aligned} \quad (8)$$

where E_{u1} and E_{u2} are the unloading moduli form the outer and inner surfaces, respectively.

Figure 8 shows the deformation pattern for 'LA', where both inner and outer surfaces are plastic, and assuming that $E_{u1} = E_{u2} = E_{un}$, the amount of springback is

$$\begin{aligned} SB &= \frac{\varepsilon_l - \varepsilon_u}{\varepsilon_l} = \frac{\sigma_{u1}/E_{u1} - \sigma_{u2}/E_{u2}}{\varepsilon_l} \\ &= \frac{K(t/2\rho + \varepsilon_a)^n + K(t/2\rho - \varepsilon_a)^n}{(t/\rho) \cdot E_{un}} \\ &= \frac{K\rho[(t/2\rho + \varepsilon_a)^n + (t/2\rho - \varepsilon_a)^n]}{tE_{un}} \end{aligned} \quad (9)$$

where the strength of the sheet on the outer surface is $\sigma_{u1} = K(t/2\rho + \varepsilon_a)^n$ and the strength of the sheet on the inner surface is $\sigma_{u2} = -K(t/2\rho - \varepsilon_a)^n$.

Figure 9 shows the deformation pattern for 'LB', where the inner surface is elastic and the outer

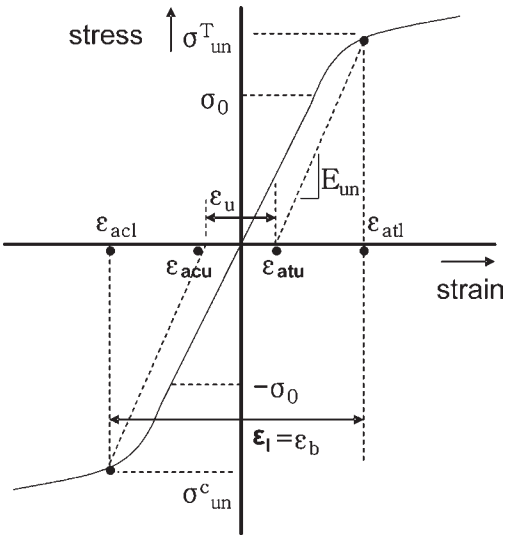

Fig. 8 Stress–strain distribution for deformation pattern LA

surface is plastic, and the amount of springback is

$$SB = \frac{\varepsilon_l - \varepsilon_u}{\varepsilon_l} = \frac{\varepsilon_l - (\varepsilon_a + t/2\rho - \sigma_{un}/E_{un})}{\varepsilon_l} \quad (10)$$

as $\varepsilon_l = \varepsilon_b = t/\rho$, therefore

$$SB = \frac{t + 2\rho(\sigma_{un}/E_{un} - \varepsilon_a)}{2t} \quad (11)$$

where $\sigma_{un} = K(t/2\rho + \varepsilon_a)^n$

Figure 10 shows the deformation pattern for 'LC', where both inner and outer surfaces are plastic and

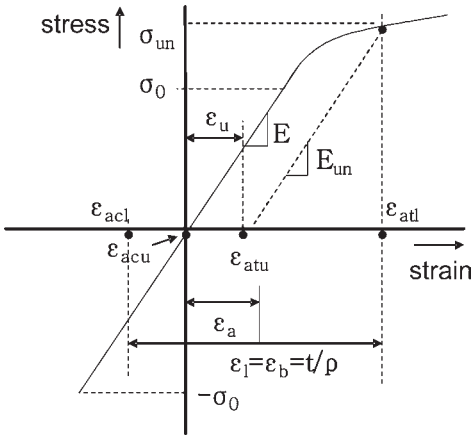

Fig. 9 Stress–strain distribution for deformation pattern LB

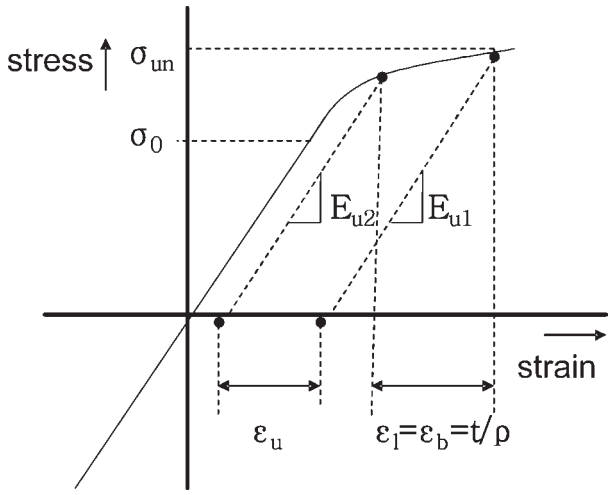

Fig. 10 Stress–strain distribution for deformation pattern LC

the amount of springback is

$$\begin{aligned} \mathrm{SB} &= \frac{\varepsilon_\mathrm{l} - \varepsilon_\mathrm{u}}{\varepsilon_\mathrm{l}} \\ &= \frac{t/\rho - (\varepsilon_\mathrm{a} + t/2\rho - K(\varepsilon_\mathrm{a} + t/2\rho)^n/E_{\mathrm{u1}} - [\varepsilon_\mathrm{a} - t/2\rho - K(\varepsilon_\mathrm{a} - t/2\rho)^n/E_{\mathrm{u2}}])}{\varepsilon_\mathrm{l}} \\ &= \frac{K\rho[(\varepsilon_\mathrm{a} + t/2\rho)^n/E_{\mathrm{u1}} - (\varepsilon_\mathrm{a} - t/2\rho)^n/E_{\mathrm{u2}}]}{t} \end{aligned} \tag{12}$$

2.2 Springback model based on bending moment

To compare the residual differential strain model derived in the previous section, a second analytical model based on the bending moment [**14**, **15**] is derived for the same six deformation patterns. The bending moment model is the traditional analytical model used to determine springback. The bending moment model depends on the unloading from an applied moment in the sheet, causing a change in the curvature of the bend.

When a normal section of unit width of the sheet is bent, a stress distribution due to bending occurs. Tension, T, on the sheet causes a change in the stress distribution, such that T will balance the integral of the stress distribution due to static equilibrium. The bending moment can be obtained by finding the first moment of the stress distribution. By examining analytical expressions for the tension, T, and the bending moment, M, the springback can be obtained.

From the moment at a given condition before unloading

$$M_\mathrm{s} = I \cdot E \cdot \left(\frac{1}{\rho}\right) \tag{13}$$

where subscript s indicates the start of the unloading process, I the moment of inertia and $1/\rho$ the curvature in the sheet caused by the moment.

ρ will change as the moment changes, so

$$\Delta M = I \cdot E \cdot \Delta\left(\frac{1}{\rho}\right) \tag{14}$$

Extraction of the sheet from a die means $M_\mathrm{f} = 0$, where the subscript f indicates the finish of the unloading process. Therefore, during unloading

$$\Delta M = M_\mathrm{f} - M_\mathrm{s} = 0 - M_\mathrm{s} = -M_\mathrm{s} \tag{15}$$

The change in the bending radius is

$$\Delta\left(\frac{1}{\rho}\right) = \left(\frac{1}{\rho}\right)_\mathrm{f} - \left(\frac{1}{\rho}\right)_\mathrm{s} = \frac{\Delta M}{I \cdot E} = -\frac{M_\mathrm{s}}{I \cdot E} = \Delta\theta \tag{16}$$

where $\Delta\theta$, the angular change, is the measure of the springback.

For a rectangular sheet cross-section, the moment of inertia per unit width (i.e. $w = 1$) is

$$I = w \cdot \frac{t^3}{12} = \frac{t^3}{12} \tag{17}$$

Therefore

$$\Delta\theta = \Delta\left(\frac{1}{\rho}\right) = \left(\frac{1}{\rho}\right)_\mathrm{f} - \left(\frac{1}{\rho}\right)_\mathrm{s} = -\frac{12 \cdot \mathrm{M_s}}{E \cdot t^3} \tag{18}$$

Figure 11 shows the deformation pattern for SA where both inner and outer surfaces are elastic.

Tension T for the deformation pattern for SA is

$$\begin{aligned} T &= \int_{-t/2}^{t/2} \left[\frac{E}{\rho}\left(\frac{2a-1}{2}\right) \cdot t + \frac{E}{\rho} \cdot y\right] \cdot \mathrm{d}y \\ &= \frac{E(2a-1) \cdot t^2}{2\rho} \end{aligned} \tag{19}$$

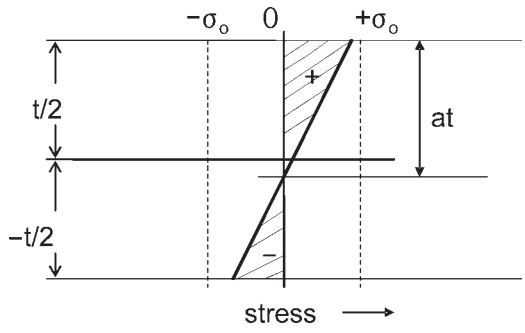

Fig. 11 Stress distribution for deformation pattern SA

where, for this deformation pattern, a is the normalized distance between the outer surface of the sheet and the neutral plane.

Moment, M, for the deformation pattern SA is

$$M = \int_{-t/2}^{t/2} \left[\frac{E}{\rho}\left(\frac{2a-1}{2}\right)\cdot t + \frac{E}{\rho}\cdot y\right]\cdot y \cdot \mathrm{d}y = \frac{E}{3\rho}\left[\frac{t^3}{8} - \left(-\frac{t^3}{8}\right)\right] = \frac{E\cdot t^3}{12\rho} \tag{20}$$

From equation (16), the springback is

$$\mathrm{SB} = \frac{(1/\rho)_\mathrm{s} - (1/\rho)_\mathrm{f}}{(1/\rho)_\mathrm{s}} = \frac{12M}{(1/\rho)_\mathrm{s} E t^3} \tag{21}$$

Note that equation (21) is a different equation for springback when compared with the definition given in the residual differential strain model in equation (4). The difference is due to the fact that the traditional bending moment model relies on the moment–curvature relationship and defines springback in terms of angular change as in equation (16). As the springback measure for both models is determined on a percentage basis and both models account for the elastic unloading after bending, a comparison between the two models can be made despite the differences between the two definitions.

Figure 12 shows the deformation pattern for SB, where the inner surface is elastic and the outer surface is plastic.

Tension T for the deformation pattern for SB is

$$T = \int_{t/2-at}^{t/2} \sigma\cdot \mathrm{d}y + \frac{1}{2}\cdot\sigma_0^2\cdot\frac{\rho}{E} + \frac{1}{2}\left(\sigma_0 - \frac{E\cdot b\cdot t}{\rho}\right)\cdot\left(bt - \frac{\sigma_0\cdot\rho}{E}\right) = \frac{\rho\cdot K}{n+1}\left\{\left(\frac{t}{2\rho}+\varepsilon_\mathrm{a}\right)^{n+1} - \left[\frac{(1-2a)\cdot t}{2\rho}+\varepsilon_\mathrm{a}\right]^{n+1}\right\} - \frac{E\cdot b^2\cdot t^2}{2\rho} + \sigma_0\cdot b\cdot t \tag{22}$$

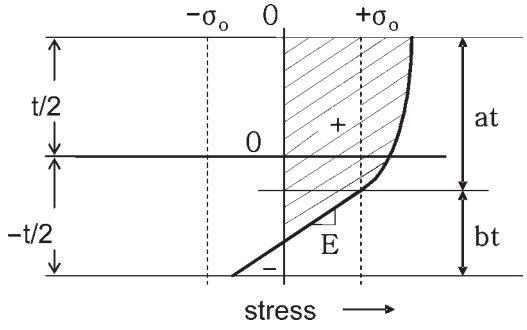

Fig. 12 Stress distribution for deformation pattern SB

where, for this deformation pattern, a is the normalized distance between the outer surface and the plane in the sheet at the yield strength and b is the normalized distance between the plane in the sheet at the yield strength and the bottom surface. In this case, $a + b = 1$.

Moment M for the deformation pattern for SB is

$$M = \int_{(1/2-a)t}^{t/2} \sigma\cdot y\cdot \mathrm{d}y + \int_{-t/2}^{(1/2-a)t}\left\{\frac{E}{\rho}\cdot y + \sigma_0 - \left(\frac{2b-1}{2}\right)\cdot\frac{t\cdot E}{\rho}\right\}\cdot y\cdot \mathrm{d}y = \frac{K\cdot\rho^2}{n+2}\left\{\left(\frac{t}{2\rho}+\varepsilon_\mathrm{a}\right)^{n+2} - \left[\frac{(1-2a)\cdot t}{2\rho}+\varepsilon_\mathrm{a}\right]^{n+2}\right\} - \frac{K\cdot\rho^2\cdot\varepsilon_\mathrm{a}}{n+1}\left\{\left(\frac{t}{2\rho}+\varepsilon_\mathrm{a}\right)^{n+1} - \left[\frac{(1-2a)\cdot t}{2\rho}+\varepsilon_\mathrm{a}\right]^{n+1}\right\} + \frac{E}{3\rho}\left[\left(\frac{1-2a}{2}\right)^3\cdot t^3 + \frac{t^3}{8}\right] + \frac{\sigma_0}{2}\left[\left(\frac{1-2a}{2}\right)^2\cdot t^2 - \frac{t^2}{4}\right] - \left(\frac{2b-1}{4}\right)\cdot\frac{E\cdot t}{\rho}\cdot\left[\left(\frac{1-2a}{2}\right)^2\cdot t^2 - \frac{t^2}{4}\right] \tag{23}$$

From equation (18), the springback is

$$\mathrm{SB} = \frac{(1/\rho)_\mathrm{s} - (1/\rho)_\mathrm{f}}{(1/\rho)_\mathrm{s}} = \frac{12M}{(1/\rho)_\mathrm{s} E t^3} \tag{24}$$

Figure 13 shows the deformation pattern for SC, where both the inner and outer surfaces are plastic.

Tension T for the deformation pattern for SC is

$$T = \int_{-t/2}^{t/2} \sigma\cdot\mathrm{d}y = \int_{-t/2}^{t/2} K\cdot\left(\frac{y}{\rho}+\varepsilon_\mathrm{a}\right)^n\cdot\mathrm{d}y = \frac{\rho\cdot K}{n+1}\cdot\left[\left(\frac{t}{2\rho}+\varepsilon_\mathrm{a}\right)^{n+1} - \left(-\frac{t}{2\rho}+\varepsilon_\mathrm{a}\right)^{n+1}\right] \tag{25}$$

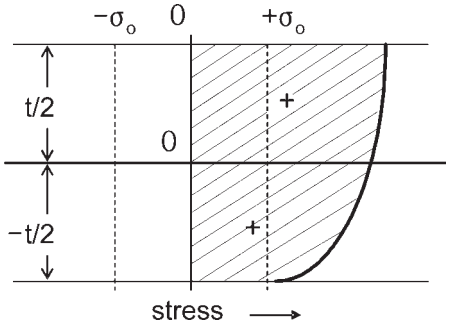

Fig. 13 Stress distribution for deformation pattern SC

Moment M for the deformation pattern for SC is

$$M = \int_{-t/2}^{t/2} \sigma \cdot y \cdot \mathrm{d}y = \int_{-t/2}^{t/2} K \cdot \left(\frac{y}{\rho} + \varepsilon_a\right)^n \cdot y \cdot \mathrm{d}y$$
$$= \frac{\rho^2 \cdot K}{n+2}\left[\left(\frac{t}{2\rho} + \varepsilon_a\right)^{n+2} - \left(-\frac{t}{2\rho} + \varepsilon_a\right)^{n+2}\right]$$
$$- \frac{\rho^2 \cdot K}{n+1}\left[\left(\frac{t}{2\rho} + \varepsilon_a\right)^{n+1} - \left(-\frac{t}{2\rho} + \varepsilon_a\right)^{n+1}\right] \quad (26)$$

The springback can be obtained from equation (24).

Figure 14 shows the deformation pattern for LA, where both the inner and outer surfaces are plastic.

Tension T for the deformation pattern for LA is

$$T = \int_{t/2-at}^{t/2} \sigma \cdot \mathrm{d}y + \frac{1}{4} \cdot \sigma_0 \cdot b \cdot t - \frac{1}{4} \cdot \sigma_0 \cdot b \cdot t$$
$$- \int_{(2a+2b-1)/2 \cdot t}^{t/2} \sigma \cdot \mathrm{d}y$$
$$= \frac{\rho \cdot K}{n+1}\left\{\left(\frac{t}{2\rho} + \varepsilon_a\right)^{n+1} - \left[\frac{(1-2a) \cdot t}{2\rho} + \varepsilon_a\right]^{n+1}\right\}$$
$$- \frac{\rho \cdot K}{n+1}\left\{\left(\frac{t}{2\rho} - \varepsilon_a\right)^{n+1}\right.$$
$$\left. - \left[\frac{(2a+2b-1) \cdot t}{2\rho} - \varepsilon_a\right]^{n+1}\right\} \quad (27)$$

where, for this deformation pattern, a is the normalized distance between the outer surface and the plane in the sheet at the yield strength and b is the normalized distance between the first plane in the sheet at the yield strength and the second plane in the sheet at the yield strength.

Moment M for the deformation pattern for LA is

$$M = \int_{(1-2a/2) \cdot t}^{t/2} \sigma \cdot y \cdot \mathrm{d}y + \int_{(1-2a-2b/2) \cdot t}^{(1-2a/2) \cdot t} \left[\frac{2 \cdot \sigma_0 \cdot y}{b \cdot t}\right.$$
$$\left. + \sigma_0\left(\frac{b+2a-1}{b}\right)\right] \cdot y \cdot \mathrm{d}y + \int_{(1-2a-2b/2) \cdot t}^{-t/2} \sigma \cdot y \cdot \mathrm{d}y$$
$$= \frac{\rho^2 \cdot K}{n+2}\left\{\left(\frac{t}{2\rho} + \varepsilon_a\right)^{n+2} - \left[\frac{(1-2a) \cdot t}{2\rho} + \varepsilon_a\right]^{n+2}\right\}$$
$$- \frac{K \cdot \rho^2 \cdot \varepsilon_a}{n+1}\left\{\left(\frac{t}{2\rho} + \varepsilon_a\right)^{n+1} - \left[\frac{(1-2a) \cdot t}{2\rho} + \varepsilon_a\right]^{n+1}\right\}$$
$$+ \frac{2 \cdot \sigma_0}{3 \cdot b \cdot t}\left(\frac{1}{2} - a\right)^3 \cdot t^3 + \frac{\sigma_0 \cdot (b+2a-1)}{2b} \cdot \left(\frac{(1-2a)}{2}\right)^2 \cdot t^2$$
$$- \frac{2 \cdot \sigma_0}{3 \cdot b \cdot t}\left(\frac{1}{2} - a - b\right)^3 \cdot t^3 - \frac{\sigma_0(b+2a+1)}{2b}$$
$$\cdot \left(\frac{1-2a-2b}{2}\right)^2 \cdot t^2$$
$$+ \frac{\rho^2 \cdot K}{n+2}\left\{\left(\frac{t}{2\rho} - \varepsilon_a\right)^{n+2} - \left[\frac{(2a+2b-1) \cdot t}{2\rho} - \varepsilon_a\right]^{n+2}\right\}$$
$$- \frac{K \cdot \rho^2 \cdot \varepsilon_a}{n+1}\left\{\left(\frac{t}{2\rho} - \varepsilon_a\right)^{n+1}\right.$$
$$\left. - \left[\frac{(2a+2b-1) \cdot t}{2\rho} - \varepsilon_a\right]^{n+1}\right\} \quad (28)$$

The springback can be obtained from equation (24).

Figure 15 shows the deformation pattern for LB, where the inner surface is elastic and the outer surface is plastic.

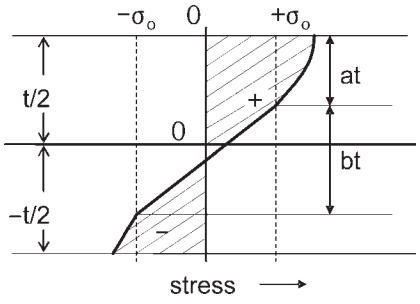

Fig. 14 Stress distribution for deformation pattern LA

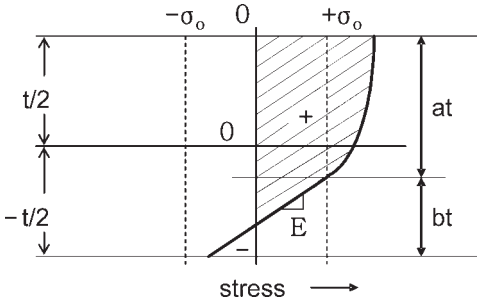

Fig. 15 Stress distribution for deformation pattern LB

Tension, T for the deformation pattern for LB is

$$T = \int_{t/2-at}^{t/2} \sigma \cdot \mathrm{d}y + \frac{1}{2} \cdot \sigma_0^2 \cdot \frac{\rho}{E} + \frac{1}{2}\left(\sigma_0 - \frac{E \cdot b \cdot t}{\rho}\right) \cdot \left(bt - \frac{\sigma_0 \cdot \rho}{E}\right)$$
$$= \frac{\rho \cdot K}{n+1}\left\{\left(\frac{t}{2\rho} + \varepsilon_a\right)^{n+1} - \left[\frac{(1-2a)\cdot t}{2\rho} + \varepsilon_a\right]^{n+1}\right\} - \frac{E \cdot b^2 \cdot t^2}{2\rho} + \sigma_0 \cdot b \cdot t \quad (29)$$

where, for this deformation pattern, a is the normalized distance between the outer surface and the plane in the sheet at the yield strength and b is the normalized distance between the plane in the sheet at the yield strength and the bottom surface. In this case, $a + b = 1$.

Moment M for the deformation pattern for LB is:

$$M = \int_{(1/2-a)t}^{t/2} \sigma \cdot y \cdot \mathrm{d}y + \int_{-t/2}^{(1/2-a)t} \left\{\frac{E}{\rho} \cdot y + \sigma_0 - \left(\frac{2b-1}{2}\right) \cdot \frac{t \cdot E}{\rho}\right\} \cdot y \cdot \mathrm{d}y$$
$$= \frac{K \cdot \rho^2}{n+2}\left\{\left(\frac{t}{2\rho} + \varepsilon_a\right)^{n+2} - \left[\frac{(1-2a)\cdot t)}{2\rho} + \varepsilon_a\right]^{n+2}\right\} - \frac{K \cdot \rho^2 \cdot \varepsilon_a}{n+1}\left\{\left(\frac{t}{2\rho} + \varepsilon_a\right)^{n+1} - \left[\frac{(1-2a)\cdot t}{2\rho} + \varepsilon_a\right]^{n+1}\right\}$$
$$+ \frac{E}{3\rho}\left[\left(\frac{1-2a}{2}\right)^3 \cdot t^3 + \frac{t^3}{8}\right] + \frac{\sigma_0}{2}\left[\left(\frac{1-2a}{2}\right)^2 \cdot t^2 - \frac{t^2}{4}\right] - \left(\frac{2b-1}{4}\right) \cdot \frac{E \cdot t}{\rho} \cdot \left[\left(\frac{1-2a}{2}\right)^2 \cdot t^2 - \frac{t^2}{4}\right] \quad (30)$$

The springback can be obtained from equation (24).

Figure 16 shows the deformation pattern for LC, where both inner and outer surfaces are plastic.

Tension T for the deformation pattern for LC is:

$$T = \int_{-t/2}^{t/2} \sigma \cdot \ \mathrm{d}y = \int_{-t/2}^{t/2} K \cdot \left(\frac{y}{\rho} + \varepsilon_a\right)^n \cdot \mathrm{d}y$$
$$= \frac{\rho \cdot K}{n+1} \cdot \left[\left(\frac{t}{2\rho} + \varepsilon_a\right)^{n+1} - \left(-\frac{t}{2\rho} + \varepsilon_a\right)^{n+1}\right] \quad (31)$$

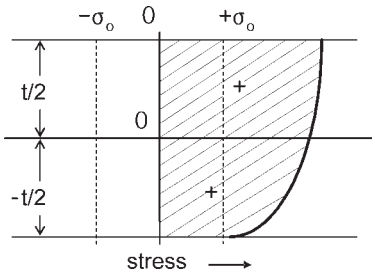

Fig. 16 Stress distribution for deformation pattern LC

Moment M for the deformation pattern for LC is

$$M = \int_{-t/2}^{t/2} \sigma \cdot y \cdot \mathrm{d}y = \int_{-t/2}^{t/2} K \cdot \left(\frac{y}{\rho} + \varepsilon_a\right)^n \cdot y \cdot \mathrm{d}y$$
$$= \frac{\rho^2 \cdot K}{n+2}\left[\left(\frac{t}{2\rho} + \varepsilon_a\right)^{n+2} - \left(-\frac{t}{2\rho} + \varepsilon_a\right)^{n+2}\right] - \frac{\rho^2 \cdot K}{n+1}\left[\left(\frac{t}{2\rho} + \varepsilon_a\right)^{n+1} - \left(-\frac{t}{2\rho} + \varepsilon_a\right)^{n+1}\right] \quad (32)$$

The springback can be obtained from equation (24).

3 RESULTS AND DISCUSSION

To evaluate the two models developed in this study, four materials were selected for comparison. The materials used were a mild steel (SCP-1), two advanced high strength steels (DP780 and TRIP780), and an aluminium alloy (Al2008). Figure 17 shows the stress–strain relationships for these materials. Table 3 gives the specific tensile properties for the materials, which are required as input for the models.

Model evaluations were made for sheet thicknesses of 0.7, 1.0, 1.4, 1.7, and 2.0 mm and bending die radii of 3.175, 6.35, 9.525, 12.7, and 25.4 mm.

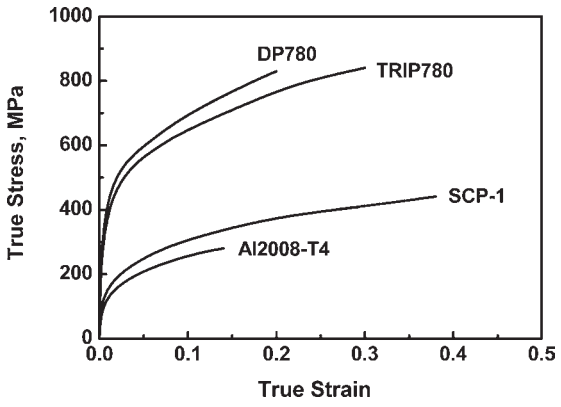

Fig. 17 True stress–true strain curves

Table 3 Tensile properties of model materials

Material	Elastic modulus (MPa)	Yield strength (MPa)	Tensile strength (MPa)	Strength coefficient K (MPa)	n	ϵ_f
Al 2008	71 000	120	210	490	0.26	13.9
SCP-1	2 06 000	160	394	567	0.264	39.0
TRIP 780	2 06 000	470	785	1108	0.228	30.0
DP 780	2 06 000	481	843	1200	0.230	19.5

To assess the effect of applied strain (stress), approximately ten different values of ε_a were used. The range of these applied strain values spanned the various deformation patterns given in Tables 1 and 2.

The values for the parameters a and b in the bending moment model are determined by calculating tension (T) and are then used in the bending moment calculation.

When the applied strain, ε_a, is in the elastic range, the tension (T) in the bending moment model is calculated as

$$T = t\sigma_a = tE\varepsilon_a \tag{33}$$

When the applied strain is in the plastic range, the tension (T) in the bending moment model is calculated as

$$T = t\sigma_a = tK(\varepsilon_a)^n \tag{34}$$

Figure 18 shows the predicted springback using the residual differential strain model (solid lines) and the bending moment model (dotted lines) for two different combinations of thickness–bending radius of curvature. With increasing applied strain (ε_a), the predicted amount of springback undergoes significant change. In both models, mild steel (SCP-1) exhibits the lowest amount of springback, whereas the aluminium sheet (Al2008) has the largest amount of springback. The advanced high strength steels also show significantly higher springback than mild steel, with the dual phase steel, DP780, exhibiting higher springback than TRIP780. Both models sort the materials in the same order with respect to springback.

For the bending moment model, the springback gradually decreases with increasing applied strain (ε_a), whereas the residual differential strain model shows only a slight decrease until the applied strain (i.e. applied tension) reaches a transition value. When the applied strain reaches the transition

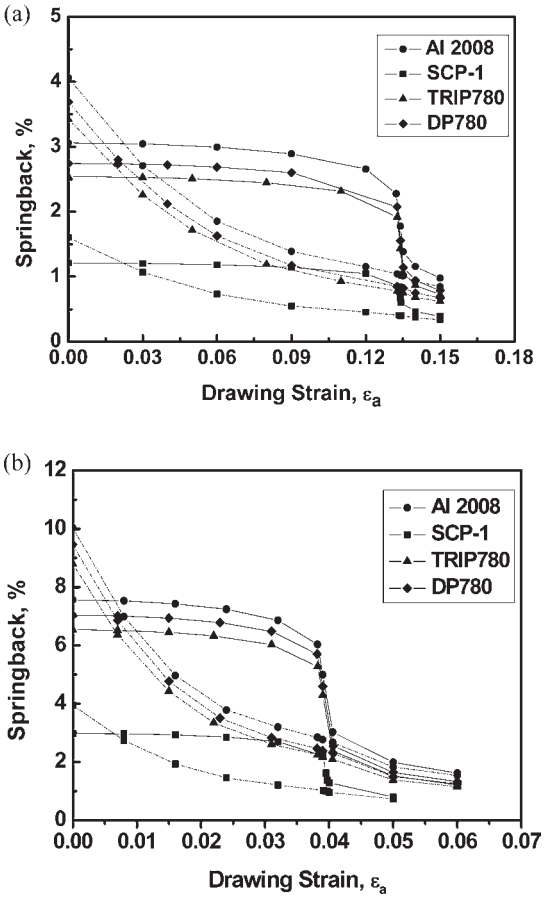

Fig. 18 Comparison of predicted springback between residual differential strain model (solid lines) and the bending moment model (dotted lines) for (a) thickness = 1.7 mm, $\rho = 6.35$ mm and (b) thickness = 1.0 mm, $\rho = 12.7$ mm

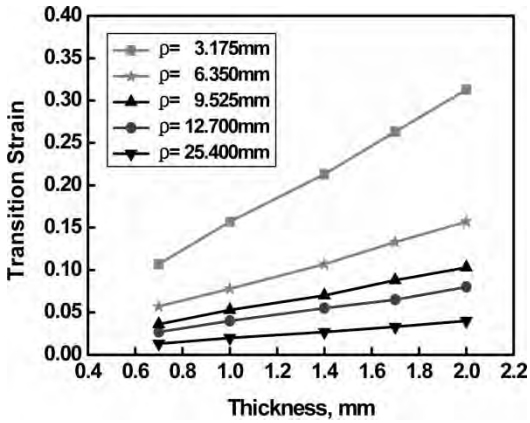

Fig. 19 The applied strain transition for the model based on residual differential strain

value, then the springback decreases rapidly and merges with the model based on the bending moment. The transition values for the applied strain, as shown in Fig. 19, increase with increasing thickness and decreasing radius of curvature (ρ). This transition behaviour occurs because the elastic–plastic behaviour of sheet metal has three distinct valid ranges.

Figure 20 compares the variation of springback with sheet thickness at different radii of curvatures without any applied tension ($\varepsilon_a = 0$). The amount of springback decreases with increasing thickness, and the slopes of the curves calculated from both models show similar trends. Figure 21 compares the variation of springback with radii of curvatures at different sheet thicknesses without any applied

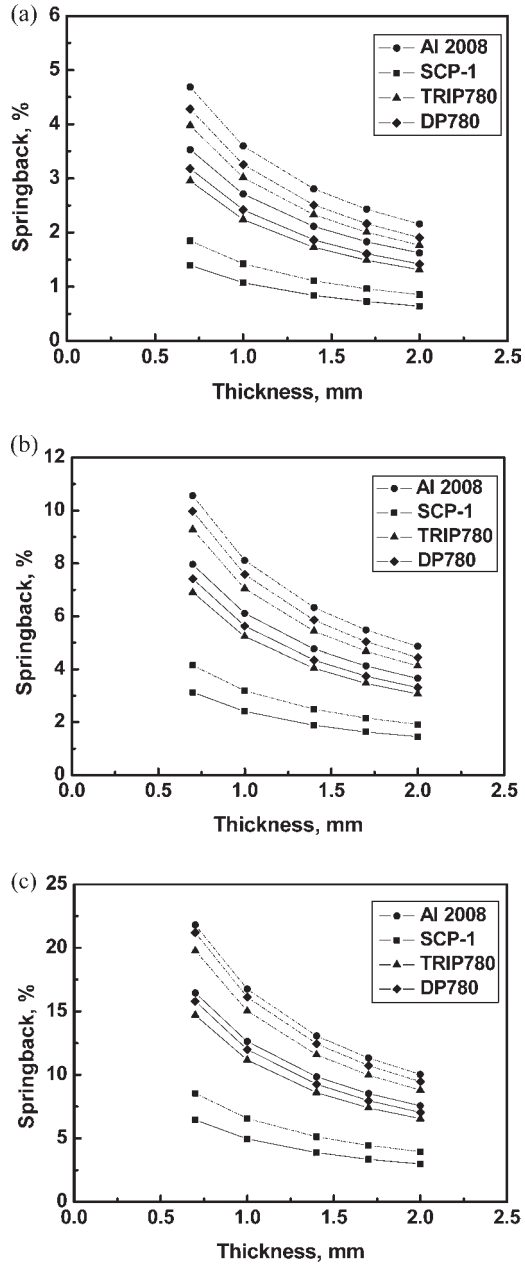

Fig. 20 Variation of springback with thickness for the residual differential strain model (solid lines) and the bending moment model (dotted lines) for (a) curvature radius = 3.175 mm, (b) curvature radius = 9.525 mm, and (c) curvature radius = 25.4 mm

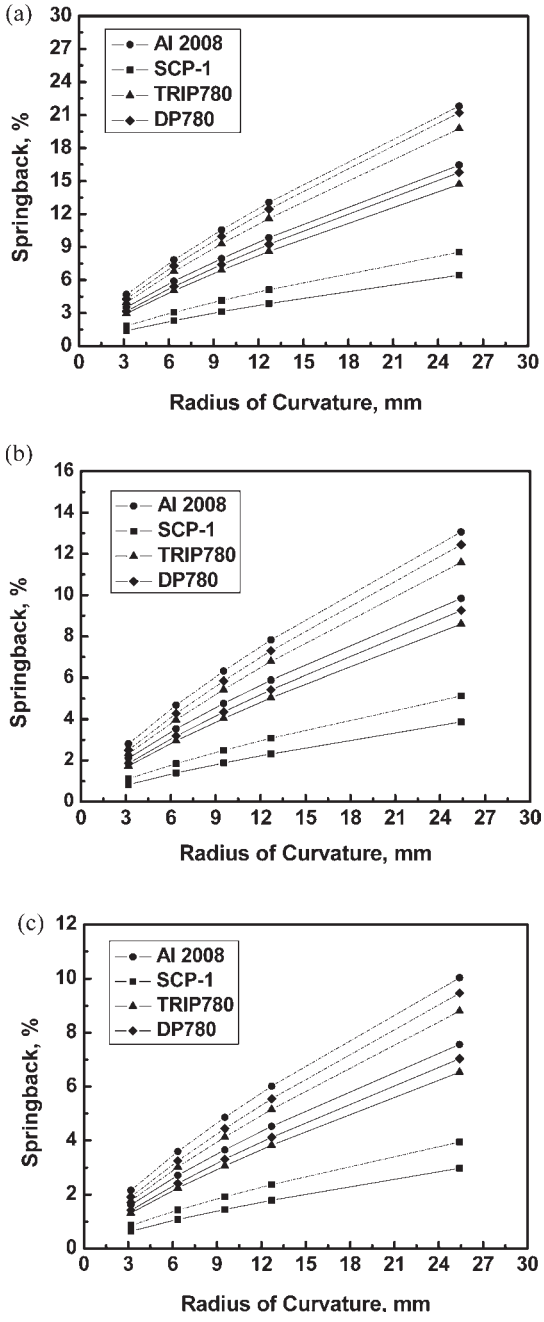

Fig. 21 Variation of springback with radius of curvature for the residual differential strain model (solid lines) and bending moment model (dotted lines) for (a) thickness = 0.7 mm, (b) thickness = 1.4 mm, and (c) thickness = 2.0 mm

tension ($\varepsilon_a = 0$). The amount of springback increases with increasing radius of curvature, and the slopes of the curves from both models also show similar trends. According to the evaluation results, the model based on bending moments predicts ~25 per cent higher springback values than those of models based on residual differential strain for zero applied tension.

The residual differentials strain model that has been derived in this study, appears to provide a reasonable estimate of springback when compared to the traditional bending moment model, especially when the amount of applied tension is sufficiently high. The residual differential strain model produces equations, which are simpler than the bending moment model. Experimental verification for both of these models is still required.

4 SUMMARY

The analysis of the springback of sheet metal during bending to a radius with applied tensile strain requires the use of six different deformation patterns. These patterns are elastic–elastic, plastic–elastic, and plastic–plastic for the outer and inner surfaces when $\sigma_0/E \geqslant t/2\rho$ and plastic–plastic with an elastic core, elastic–plastic, and plastic–plastic for the inner and outer surfaces when $t/2\rho \geqslant \sigma_0/E$. Two different analytical models for springback have been derived. The new model, which is the residual differential strain model, uses strain differences between the outer and inner surfaces of greatest radius prior to unloading and after elastic recovery as a measure of springback. The strains on the outer and inner surfaces are calculated for the loaded condition and after elastic recovery under the six different deformation patterns. The second model, which is the traditional bending moment model, uses the curvature differences between the loaded and unloaded conditions as a measure of springback. The moment and the tension within the strip are calculated for the loaded condition. From the moment in the strip, the amount of springback can be determined.

Both models have been compared using four different materials – a low carbon steel, two advanced high strength steels, and an aluminium alloy. The residual differential strain model has an applied transition strain, where the springback undergoes a dramatic decrease. Both models show that springback decreases with increased strip thickness and with decreased radius of curvature. For no applied tension, the bending moment model predicts about 25% more springback when compared with the residual differential strain model. Experimental verification of the models is still required.

ACKNOWLEDGEMENT

This work was partially supported by a grant from the National Core Research Center (NCRC) program funded by the Korea Science and Engineering Foundation (KOSEF).

REFERENCES

1 **Huang, H. M., Liu, S. D.,** and **Jiang, S.** Stress and strain histories of multiple bending–unbending springback process. *Trans. ASME, J. Eng. Mater. and Technol.*, 2001, **123**, 384–390.
2 **Seo, D. G., Chang, S. H.,** and **Lee, S. M.** Springback characteristics of steel sheets for warm U-draw bending. *Metals Mater. Int.*, 2003, **9**, 497–501.
3 **D'Acquisto, L.** and **Fratini, L.** Springback effect evaluation in three-dimensional stamping processes at the varying blank holder force. *J. Mech. Eng. Sci.*, 2006, **220**, 1827–1837.
4 **Carden, W. D., Geng, L. M., Matlock, D. K.,** and **Wagnor, R. H.** Measurement of springback. *Int. J. Mech. Sci.*, 2002, **44**, 79–101.
5 **Michael, D. T.** and **Henrik, A.** ULSAB-advanced vehicle concepts – overview and design. SAE Paper 2002-01-0036, 2002.
6 **Paul, G. S.** ULSAB-advanced vehicle concepts – manufacturing and processes. SAE Paper 2002-01-0039, 2002.
7 **Reitman, B., Kose, K., Ohnimus, S., Petzoldt, M.,** and **Weiher, J.** Recent advances in industrial applied numerical aided springback compensation, In Proceedings of IDDRG International Deep Drawing Research Group 2004 Conference, Stahl Institute VDEh, Germany, 2004, pp. 38–44.
8 **Schönback, É., Glanzer, G., Kubli, W.,** and **Selig, M.** Springback simulation – the last missing link for a complete forming simulation. In Proceedings of IDDRG International Deep Drawing Research Group 2004 Conference, Stahl Institute VDEh, Germany, 2004, pp. 83–94.
9 **Papeleux, L.** and **Ponthot, J.-P.** Finite element simulation of springback in sheet metal forming. *J. Mater. Process. Technol.*, 2002 **125–126**, 785–791.
10 **Urabe, M., Yuji, Y.,** and **Hosoya, Y.** Optimization of tool configuration for press forming of high strength steel sheets by elementary elasto-plastic analysis. In Proceedings of IDDRG International Deep Drawing Research Group 2000 Conference, North American Deep Drawing Research Group, USA, 2000, pp. 127–134.
11 **Pourboghrat, F.** and **Chu, E.** Prediction of springback and side-wall curl in 2-D draw bending. *J. Mater. Process. Technol.*, 1995 **50**, 361–374.
12 **Pourboghrat, F., Karabin, M. E., Becker, R. C.,** and **Chung, K.** A hybrid membrane/shell method for calculating springback of anisotropic sheet metals undergoing axisymmetric loading. *Int. J. Plast.*, 2000, **16**, 677–700.
13 **Zhang, Z. T.** and **Lee, D.** Development of a new model for plane strain bending and springback analysis. *J. Mater. Eng. Perform.*, 1995 **4**, 291–300.

14 Thomas, G. G. *Production technology*, 1970, pp. 99–103, (Oxford University Press, London, UK).
15 Mielnik, E. M. *Metal working science and engineering*, 1991 (McGraw Hill, New York, NY, USA).
16 Marciniak, Z. and **Duncan, J. L.** *The mechanics of sheet metal forming*, 1992, pp. 68–99 (Edward Arnold, London, UK).

APPENDIX

Notation

a normalized distance through the thickness of the sheet in the moment model
b normalized distance through the thickness of the sheet in the moment model
E elastic modulus on loading
E_{un} effective elastic unloading modulus
E_{u1} effective elastic unloading modulus on the outer surface
E_{u2} effective elastic unloading modulus on the inner surface
K strength coefficient
m parameter $= y_e/(t/2)$
n strain hardening exponent
S_p springback parameter
SB springback
t thickness
y_e geometrical position of elastic–plastic transition point

ε_a axial strain in combined loading
ε_b bending strain in combined loading
ε_l axial plus bending strain differential while loaded, $\varepsilon_{axial\_bending\_loading}$ $(\varepsilon^{max}_{axial\_tensile\_loading} - \varepsilon^{max}_{axial\_compressive\_loading})$
ε_u axial plus bending strain differential after unloading, $\varepsilon_{axial\_bending\_unloading}$ $(\varepsilon^{max}_{axial\_tensile\_unloading} - \varepsilon^{max}_{axial\_compressive\_unloading})$
ε_{al} axial strain while loaded, $\varepsilon_{axial\_loading}$
ε_{au} axial strain after unloading, $\varepsilon_{axial\_unloading}$
ε_{bl} bending strain differential while loaded, $\varepsilon_{bending\_loading}$ $(\varepsilon^{max}_{tensile\_loading} - \varepsilon^{max}_{compressive\_loading})$
ε_{bu} bending strain differential after unloading, $\varepsilon_{bending\_unloading}$ $(\varepsilon^{max}_{tensile\_unloading} - \varepsilon^{max}_{compressive\_unloading})$
ε_{cl} largest compressive bending strain(on inner surface) while loaded, $\varepsilon^{max}_{compressive\_loading}$
ε_{cu} largest compressive bending strain (on inner surface) after unloading, $\varepsilon^{max}_{compressive\_unloading}$
ε_{tl} maximum tensile bending strain (on outer surface) while loaded, $\varepsilon^{max}_{tensile\_loading}$
ε_{tu} maximum tensile bending strain (on outer surface) after unloading, $\varepsilon^{max}_{tensile\_unloading}$
ε_{acl} largest axial plus compressive bending strain (on inner surface) while loaded, $\varepsilon^{max}_{axial\_compressive\_loading}$
ε_{atl} maximum axial plus tensile bending strain (on outer surface) while loaded, $\varepsilon^{max}_{axial\_tensile\_loading}$
ε_{acu} largest axial plus compressive bending strain (on inner surface) after unloading, $\varepsilon^{max}_{axial\_compressive\_unloading}$
ε_{atu} maximum axial plus tensile bending strain (on outer surface) after unloading, $\varepsilon^{max}_{axial\_tensile\_unloading}$
ρ radius of the curvature.
σ_o yield strength
σ_{un} strength of material prior to unloading
σ_{u1} strength of material on the outer surface prior to unloading
σ_{u2} strength of material on the inner surface prior to unloading